Following the Reactions of Mechanism-Based Inhibitors with β-Lactamase by Raman Crystallography†

Marion S. Helfand,‡,§ Monica A. Totir,§,|| Marianne P. Carey,|| Andrea M. Hujer,‡ Robert A. Bonomo,‡ and Paul R. Carey*,||

Research Division, Louis Stokes Cleveland Veterans Affairs Medical Center, and Departments of Biochemistry and Chemistry, Case Western Reserve University, Cleveland, Ohio 44106

Received September 23, 2003; Revised Manuscript Received October 15, 2003

ABSTRACT: The reactions between three clinically relevant inhibitors, tazobactam, sulbactam, and clavulanic acid, and SHV β-lactamase (EC 3.5.2.6) have been followed in single crystals using a Raman microscope. The data are far superior to those obtained for the enzyme in aqueous solution and allow us to identify species on the reaction pathway and to measure the rates of the accumulation and decay of these species. A key intermediate on the reaction pathway is an acyl enzyme formed between Ser70 and the lactam ring's C═O group. By using the E166A deacylation deficient variant of the enzyme, we were able to focus on the process of acyl enzyme formation. The Raman data show that all three inhibitors form an enamine-type acyl enzyme reaching maximal populations at 10, 22, and 29 min for sulbactam, clavulanic acid, and tazobactam, respectively. The enamine intermediate exhibits a characteristic and relatively intense band near 1595 cm^{-1} due to a stretching motion of the O═C−C═C−NH moiety that shifts to lower frequency upon NH ↔ ND exchange. This feature was used to follow the kinetics of enamine buildup and decay in the crystal. Quantum mechanical calculations support the assignment of the 1595 cm^{-1} band, as well as several other bands, to a *trans*-enamine species. The Raman data also demonstrate that the lactam ring opens prior to enamine formation since the lactam ring carbonyl (C═O) peak disappears prior to the appearance of the enamine 1595 cm^{-1} band. Tazobactam appears to form approximately twice as much enamine intermediate as sulbactam and clavulanic acid, which correlates with its superior performance in the clinic, a finding that may bear on future drug design.

Antibiotic resistance mediated by β-lactamase enzymes is a growing problem worldwide. Although three inhibitors of class A β-lactamase enzymes have been available clinically for a decade or more (Figure 1), fundamental questions remain regarding the precise reaction mechanisms that are important for inhibition on time scales relevant to bacterial growth and killing. This has hindered the development of new inhibitors.

The reaction mechanisms of clavulanic acid and penicillanic acid sulfone (sulbactam) have been probed by kinetic studies and the isolation of long-lived intermediates of β-lactamase. On the basis of pI, and UV, IR, MS, and NMR investigations, a reaction scheme for class A inhibition, depicted in Figure 2, has been proposed (*1*−*10*). The mechanism outlined in Figure 2 was extrapolated later to tazobactam to explain the results obtained in kinetic studies and mass spectroscopic analysis (*11*, *12*).

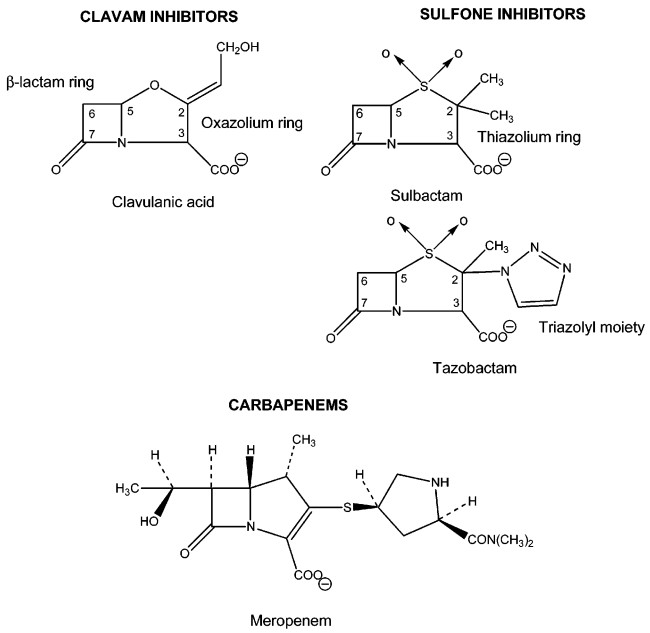

FIGURE 1: β-Lactamase inhibitors.

X-ray crystallography has revealed additional information regarding some of the intermediates observed during inhibition (*13*, *14*). These results were obtained by "soaking" an inhibitor into a single β-lactamase crystal and subsequently flash-freezing the crystal to trap any intermediate that formed.

† This work was funded by a Department of Veterans Affairs (DVA) Career Development Grant (M.S.H.), an Ohio Regents Biophotonics Initiative Grant (M.S.H., M.A.T., and P.R.C.), a DVA Merit Review Grant (A.M.H. and R.A.B.), and NIH Grant GM 54072 (P.R.C.).

* To whom correspondence should be addressed: Department of Biochemistry, Case Western Reserve University, 10900 Euclid Ave., Cleveland, OH 44106. Telephone: (216) 368-0031. E-mail: carey@biochemistry.cwru.edu.

‡ Louis Stokes Cleveland Veterans Affairs Medical Center.

§ These authors contributed equally to this work.

|| Case Western Reserve University.

10.1021/bi035716w CCC: $25.00
Published on Web 10/31/2003

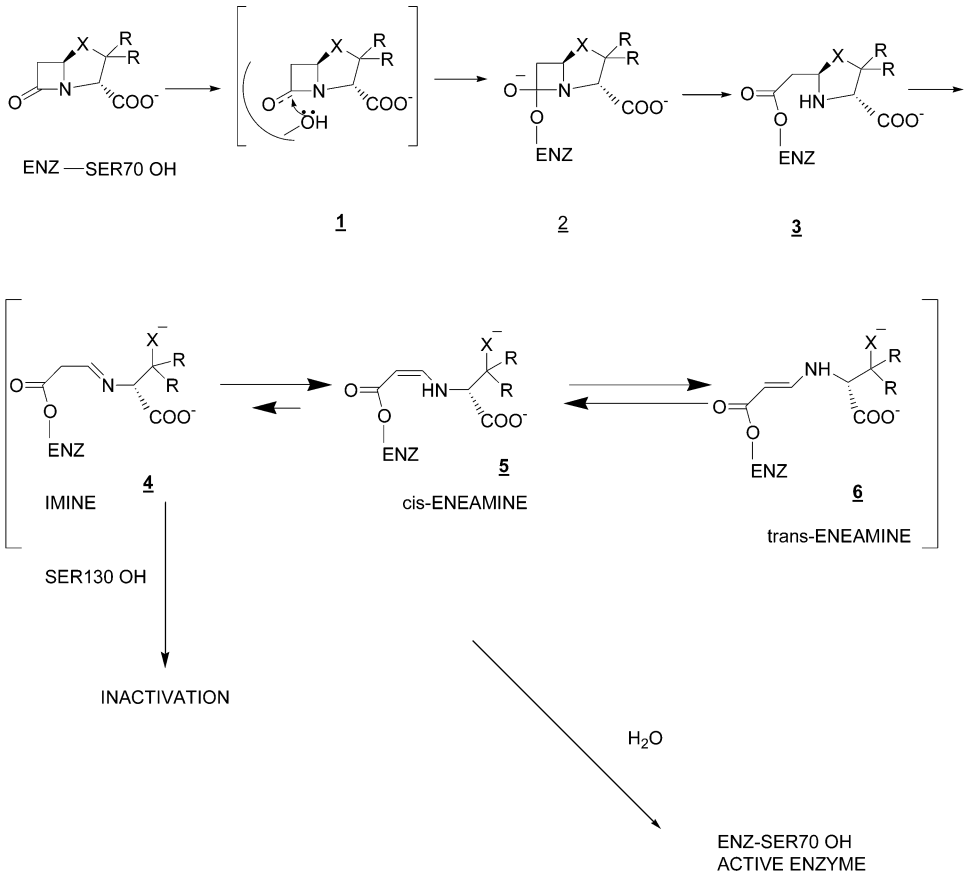

FIGURE 2: Proposed reaction mechanism for suicide inhibitors of class A β-lactamase; the reactive imine has been presumed to be the intermediate leading to permanent inactivation following loss of the $NH_2CH(COO^-)CR_2X^-$ fragment. Regeneration of the active enzyme is presumed to proceed via hydrolysis of **4**, **5**, or **6**, catalyzed by Glu166 and an active site water in the wild-type enzyme; rates for these reactions are unknown.

Unfortunately, the investigators had no independent means of assessing the progress of the reaction in the crystal to judge the optimal time for freezing. Thus, the X-ray data often revealed a mixture of species in the active site. The rates of formation and relative populations could not be estimated. These intermediates and products may or may not be relevant to inhibition of β-lactamase enzymes *in vivo* and in the clinic.

To that end, it appears that a more "real time" method, in which protein structural changes can be observed with great sensitivity and intermediates and products can be observed as they are formed, is warranted. Raman crystallography has emerged as such a tool (*15*, *16*). Raman crystallography permits the characterization of the chemical reactions between drugs that are mechanism-based inhibitors, and the SHV class A β-lactamase enzyme in single crystals. The method has several advantages over the classical Raman difference spectroscopy performed in solution; e.g., the concentrations that can be attained in the crystal result in a significantly higher *S*/*N* ratio, the spectra "sit" on a lower background prior to subtraction, and "soak in" and "soak out" experiments can be performed. The Raman difference spectrum shown in Figure 1 of the Supporting Information demonstrates these factors. This approach provides structural as well as kinetic information about intermediates, such as acyl enzymes, and products of the reaction. Since a Raman data set can be collected every 60 s, the strategy is to use Raman crystallography to map the reaction pathways for the three clinical inhibitors (Figure 1), as a function of time. By comparing the structures, populations, and kinetics of intermediates, we gain unique insights into why chemically related inhibitors behave differently. Our initial study utilizes the deacylation deficient enzyme E166A. This mutant essentially prevents regeneration of the active enzyme by blocking hydrolysis of species **4**, **5**, or **6** in Figure 2 and enables us to focus on the formation and structure of the acyl enzyme species. The results show that each inhibitor forms an α,β-unsaturated enamine intermediate on a similar time scale, but tazobactam consistently forms a larger amount of this covalently bound intermediate.

The link provided by Raman crystallography between structure, kinetics, and mechanism will also be used to guide further X-ray crystallographic studies wherein key reaction intermediates can be trapped at well-defined time points.

EXPERIMENTAL PROCEDURES

Inhibitors. Sodium clavulanate (Smith-Kline-Beecham), sulbactam (Pfizer), and tazobactam (Wyeth Pharmaceuticals) were gifts of the respective companies. Clinical grade Meropenem (Astra-Zeneca) was obtained from the Veteran Affairs pharmacy and was used without further purification. Stock solutions (20 mM) in 2 mM HEPES buffer (pH 7.0) were prepared for use with the protein crystals.

Protein Isolation and Purification. The E166A SHV clone was generated by site specific mutagenesis (*17*), and the E166A SHV variant β-lactamase protein was isolated and purified as previously described (*18*). An additional HPLC

purification step was performed using a Sephadex Hi Load 26/60 column (Pharmacia, Uppsala, Sweden) and elution with phosphate-buffered saline (pH 7.4).

Crystallization. E166A SHV was concentrated to 5 mg/mL in 2 mM HEPES buffer (pH 7.0) for crystallization using the protocol of Kuzin et al. (*19*). Briefly, crystals were prepared using the sitting drop method. Drops (volume of 10 μL) were prepared using 4 parts protein solution, 1 part 5.6 mM CYMAL-6 (Hampton Research, Laguna Niguel, CA), and 5 parts PEG-6000 (Hampton Research) (20−30%, w/v) in 0.1 M HEPES (pH 7.0). The reservoir solution consisted of PEG-6000 (20−30%, w/v) in 0.1 M HEPES (pH 7.0). Wells were sealed with packing tape and stored at room temperature. Crystals in a 2 μL drop of mother liquor solution, typically 300 μm × 300 μm × 300 μm in size, were transferred to a siliconized glass coverslip and washed four times with 0.1 M HEPES (pH 7.0) to remove excess PEG-6000 prior to use with the Raman microscope. Crystal protein concentrations were estimated to be 28 mM (J. Knox, personal communication) based on an occupancy of four molecules per unit cell and the following unit cell dimensions: a = 49.6 Å, b = 55.6 Å, and c = 87.0 Å. For experiments in D_2O, HEPES buffers were prepared using nondeuterated HEPES and titrated with NaOD to pH 6.6 (pD = pH + 0.4) (*20*). Stock solutions of inhibitors were prepared in the deuterated 2 mM HEPES buffer (pD 7.0). Protein crystals, prepared as described above, were soaked in 0.1 M deuterated HEPES buffer (pD 7.0) for 48 h to allow H−D exchange.

Raman Crystallography. The Raman microscope system has been described previously (*16*, *21*). A 647 nm Kr^+ laser beam (Innova 70 C, Coherent, Palo Alto, CA) was focused onto the protein crystals, suspended on the underside of a siliconized quartz coverslip in a 4 μL drop. Laser power (120 mW) was focused using the 20× objective to a 20 μm spot on the crystal. The crystals and the laser spot were visualized with real time color video display to ensure alignment and that no photodamage was occurring in the crystal. During data collection, spectra were acquired over 10 s intervals and 10 spectra were averaged for each acquisition time point. Spectra of the apo-β-lactamase protein crystals were obtained, followed by addition of the inhibitors to the drop to achieve a final drop volume of 4 μL and a final inhibitor concentration of 5 mM. Spectra were then acquired serially every 2−3 min following addition of inhibitor. An apo-β-lactamase spectrum was subtracted from the inhibited protein spectra at varying time intervals following addition of inhibitor, according to eq 1.

$$\text{difference spectrum} = [\text{protein}] + [\text{inhibitor}] - f[\text{protein}] \quad (1)$$

where f is a subtraction factor selected to minimize the protein amide I band from the apoprotein in the difference spectra. Typically, f has a value of 0.95−1.0. Data collection and subtractions were performed using HoloGRAMS and GRAMS/AI 7 software (ThermoGalactic, Inc., Salem, NH). Raman spectra of the inhibitors that were used were obtained under similar conditions. Spectra were obtained for 4 μL drops of inhibitor solutions prepared in 2 mM HEPES (pH 7.0) at varying inhibitor concentrations. The peak heights of various Raman bands in the inhibitor spectra were examined as a function of concentration to prepare concentration calibration curves.

Calculations. Ab initio quantum mechanical calculations were performed to predict the Raman spectra of model intermediate compounds using Gaussian 98 (*22*) software. Calculations were performed at the Hartree−Fock level using the 6-31+d(d,f) basis set.

RESULTS AND DISCUSSION

Estimating the Time for Soaking in. The Raman spectrum of a ligand bound to a protein is obtained by Raman difference spectroscopy. Thus, the Raman spectrum is recorded for an enzyme in the crystal; then the ligand is added to the surrounding solution to a final concentration of 5 mM, and after the soaking in procedure, a second spectrum is recorded for the enzyme−ligand complex. The subtraction of the Raman spectrum for the complex minus the Raman spectrum for the free enzyme is carried out using software. This yields the Raman spectrum of the bound ligand with peaks in the "positive" direction. In addition, there is often a local or global protein conformational change upon ligand binding that gives rise to protein-related features in both the positive and negative direction in the Raman difference spectrum.

For ligands that undergo chemical reactions, one complication inherent in the crystal soaking method is that the ligand reaches the enzyme molecules in the center of the crystal some time after being in contact with molecules in the outer layers. The Raman signal is collected from the focal volume of the laser beam, which is approximately 20 μm × 20 μm × 30 μm in size. When a reaction is occurring in the crystal, kinetic analysis using the Raman data is hindered by the fact that the signal is being collected from the center and from regions closer to the edge of the crystal. Thus, the validity of any kinetic analysis turns on the relative time scales of the reaction occurring between the enzyme and the β-lactam and the soaking in process. This makes it essential to measure the time it takes for the ligands to penetrate the crystal fully. Therefore, the "soak in" time was measured using the compound Meropenem (Figure 1). This compound was selected because it has an intense Raman band at 1552 cm^{-1} (C═C−C═O symmetric stretch) that can be recorded in a 25 s exposure and it is larger than the inhibitors of interest and thus sets an upper limit for the soak in time. Also, the five-membered ring remains intact during acylation, resulting in the 1552 cm^{-1} feature retaining a constant Raman intensity.

Raman difference spectra, obtained with a 25 s exposure time and recorded at 1 min intervals, reveal the immediate (<1 min) appearance of the 1552 cm^{-1} band of Meropenem, at or near maximal intensity, following addition of this β-lactam compound to the drop (Figures 2 and 3 of the Supporting Information). This demonstrates that even for large compounds, diffusion into the β-lactamase crystals occurs rapidly when compared to the time scales on which enamine chemistry occurs (see below). Moreover, there is no evidence for the β-lactam C═O vibration in the early spectra, demonstrating that acyl enzyme formation occurs in <1 min, although Meropenem has a relatively high K_M (SHV-1, 200 μM, unpublished data of C. Bethel and R. A. Bonomo).

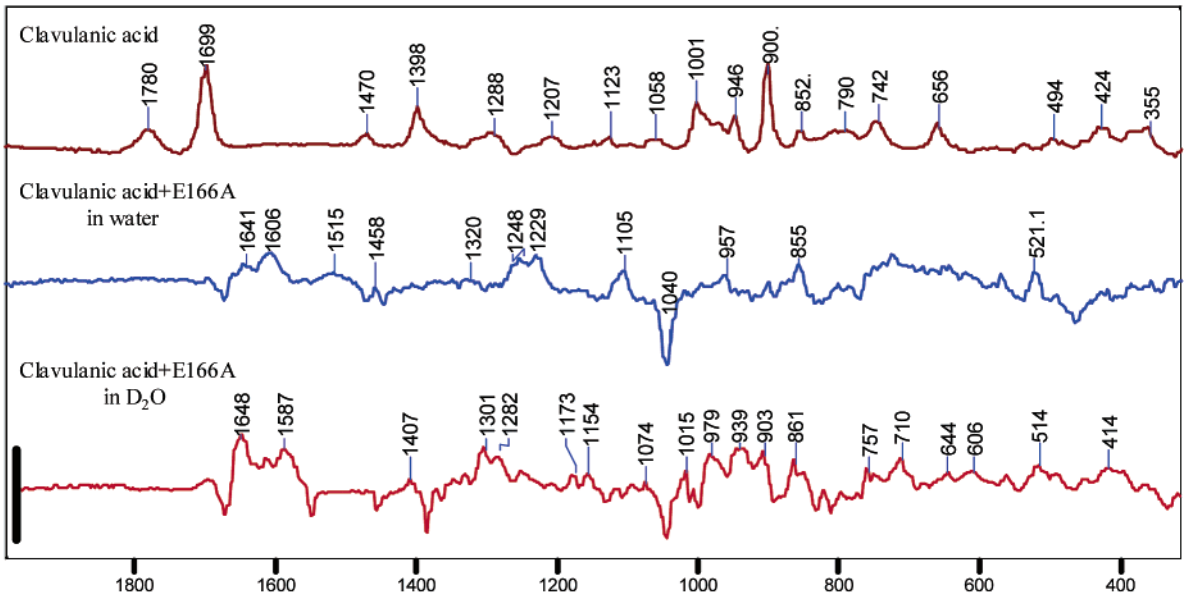

FIGURE 3: Raman difference spectra of the E166A β-lactamase crystal with clavulanic acid (middle) showing the shift of the enamine band in D_2O (bottom), both recorded 22 min after soak in. For crystal data, the vertical bar represents a 20 000 photon event. The top spectrum is the Raman spectrum of 100 mM clavulanic acid.

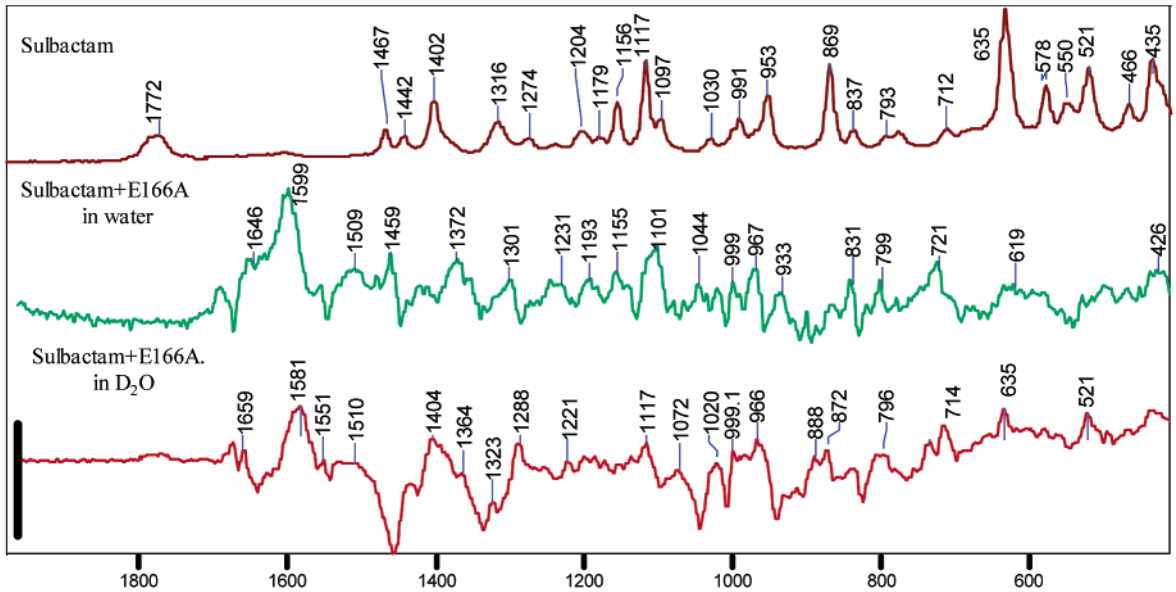

FIGURE 4: Raman difference spectra of the E166A β-lactamase crystal with sulbactam (middle) showing the shift of the enamine band in D_2O (bottom), recorded 10 and 15 min, respectively, after soak in. For crystal data, the vertical bar represents a 10 000 photon event. The top spectrum is the Raman spectrum of 100 mM sulbactam.

Raman Difference Spectra for β-Lactamase Intermediates. As the inhibitors soak into the β-lactamase crystals, they react in the active site and proceed on the reaction pathway outlined in Figure 2. However, by using the deacylation deficient variant E166A, the reaction beyond the acyl enzyme stage is very slow. Therefore, in the Raman difference spectra of the crystal complexes, we might expect to detect unreacted inhibitor, the imine, or the enamine forms of the acyl enzyme. In fact, our data are dominated by contributions from the latter species.

The Raman spectra of the free clavulanic acid, sulbactam, and tazobactam together with their Raman difference spectra as they diffuse into the crystal immersed in H_2O- and D_2O-based buffers are shown in Figures 3−5, respectively. Peaks due to the ligand or modified ligand appear in the positive direction. The general appearance of Figures 3−5 is striking. The majority of Raman modes from the free ligand are not seen in the Raman difference spectra of the complexes, following soak in. This is due to the complex chemical changes, principally ring opening, that have occurred to the ligands as outlined in Figure 2. In addition, as protein conformational changes occur due to the presence of the ligand, the Raman peaks of the protein change, resulting in the protein features appearing in Figures 3−5. They may be in either the positive or negative direction. Further features appear in the difference spectra due to the difficulty of subtracting "exactly to zero" intense peaks that are due to buffer.

Evidence of a Major Population of the Enamine Species with All of the Inhibitors. For clavulanic acid, the Raman difference spectra for the crystal complex reveal the formation of an intermediate band at 1605 cm^{-1} in water, which

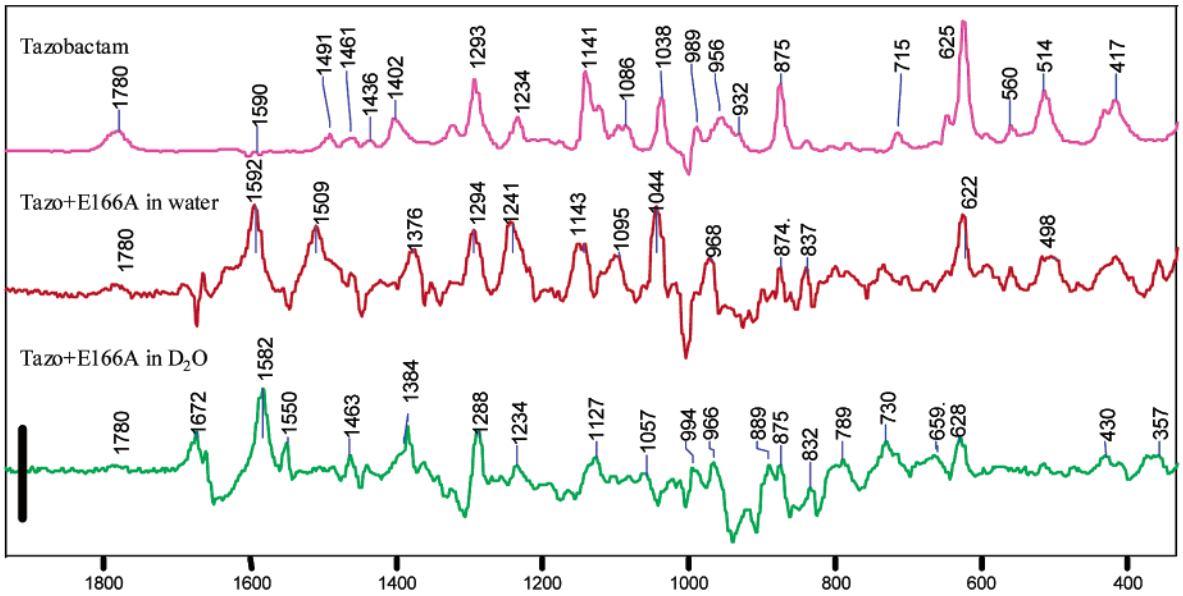

FIGURE 5: Raman difference spectra of the E166A β-lactamase crystal with tazobactam (middle) showing the shift of the enamine band in D_2O (bottom), recorded 18 and 21 min, respectively, after soak in. For crystal data, the vertical bar represents a 5000 photon event. The top spectrum is the Raman spectrum of 100 mM tazobactam.

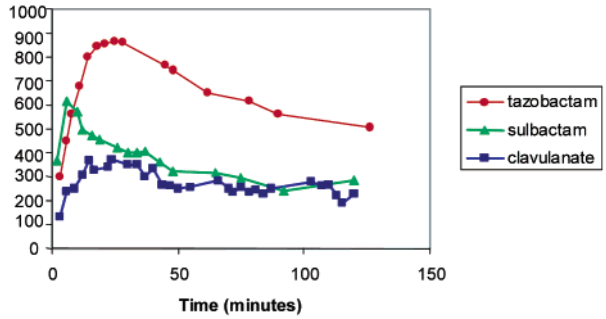

FIGURE 6: Time dependence of enamine peak height near 1595 cm^{-1} (normalized to the amide I band) for the E166A crystal and three inhibitors in H_2O.

shifts to 1587 cm^{-1} in D_2O due to NH exchange with N ↔ D, as discussed below (Figure 3). The corresponding features for sulbactam and tazobactam are seen at 1599 cm^{-1} (1581 cm^{-1} in D_2O) and 1592 cm^{-1} (1582 cm^{-1} in D_2O), respectively. The species giving rise to the 1605, 1599, and 1592 cm^{-1} features is assigned to an enamine (Figure 2) on the following basis. The enamine's conjugated O═C−C═C−NH fragment is expected to give rise to an intense Raman band in the double bond stretching region near 1600 cm^{-1}. Moreover, the totally symmetric stretch will respond to NH ↔ ND exchange, as observed. *Ab initio* calculations on the *cis*- and *trans*-enamine forms given by clavulanic acid and sulbactam confirm that the enamine has an intense Raman feature near 1600 cm^{-1}. The calculated *cis*- and *trans*-enamine stretching frequencies from sulbactam are 1582 and 1588 cm^{-1}, respectively; for clavulanic acid, these values are 1578 and 1564 cm^{-1}, respectively. The *trans* forms exhibit a 3-fold higher intensity than the *cis* isomer. Further evidence comes from the time dependence of the 1600 cm^{-1} bands seen for three reactions in Figure 6. This is consistent with the behavior of the species immediately preceding deacylation (i.e., enamine; see Figure 2). On the basis of spectroscopic data, an equilibrium between *trans*- and *cis*-enamine cannot be ruled out completely, given that *trans*-enamines are likely better Raman scatterers than *cis*-enamines. Hence, some *cis* bands may go undetected. Moreover, the imine species (Figure 2) has no conjugation and will contribute relatively little to the Raman profile, compared to the enamines. In Figures 3−5, there are other bands that track the enamine (~1595 cm^{-1}) feature's time dependence, as shown in Table 1. Thus, these are assigned to enamine modes. On the basis of *ab initio* calculations, we assign the band near 970 cm^{-1} (tazobactam and sulbactam) to the in-plane rocking of the enamine C−H bonds and the band near 700 cm^{-1} (sulbactam) to the C═C−C symmetric stretch of the enamine backbone.

For all three inhibitors, a peak appears near 1240 cm^{-1} in water that is assigned to an amide III band caused by a protein conformational change. This is likely associated with an increase in the number of peptide residues in the β Ramachandran space in a limited part of the polypeptide backbone (*23*). This assignment is supported by the disappearance of the band in D_2O and the apparent reappearance, near 960 cm^{-1}, of the region expected for deuterated amide III′. For clavulanic acid and sulbactam, the intensity of the amide III band did not appear to track that of the enamine (1595 cm^{-1}). However, for tazobactam, the time dependence for amide III and the enamine band is similar.

Evidence for Species Preceding Enamine. In the Raman difference spectra for clavulanic acid and sulbactam, there is no observable band at 1780 cm^{-1} from the C═O group in the lactam ring, once the maximal intensity for the enamine peak is attained (Figures 3 and 4). In fact, this feature cannot be seen even as the enamine peak is "growing in" within the time course shown. This is evidence that the lactam ring has opened prior to enamine formation. However, we have not detected any unique Raman features of species **4** (Figure 2). Tazobactam behaves differently in that it still has some of the carbonyl feature present in the Raman difference spectrum at the time at which the maximum intensity for the enamine band is attained (Figure 5). This can be explained by the fact that some amount of tazobactam is nonspecifically bound to the enzyme, with its lactam ring

Table 1: Raman Frequencies for the Three Inhibitors in Water, Temporally Related to the Enamine Intermediate

assignment	tazobactam frequency ($cm^{-1} \pm 5\ cm^{-1}$)	sulbactam frequency ($cm^{-1} \pm 5\ cm^{-1}$)	clavulanic acid frequency ($cm^{-1} \pm 5\ cm^{-1}$)
enamine O−C═C−N symmetric stretch	1592 in H_2O (1582 in D_2O)	1599 in H_2O (1581 in D_2O)	1605 in H_2O (1587 in D_2O)
other enamine band	969	972	
	787	727	799
			521 in H_2O (514 in D_2O)

intact. Nonspecific binding of tazobactam was also detected in the crystallographic analysis (*14*).

Kinetics of Enamine Formation. The time dependence of the main enamine peak formed with tazobactam, sulbactam, and clavulanic acid is shown in Figure 6, in which the maximal intensity values are attained at 29, 10, and 22 min, respectively.

A slow decay is observed due to slow spontaneous hydrolysis and irreversible inactivation (Figure 2). The hydrolysis is very slow since the enamine is stable during "soak out" experiments; i.e., when the inhibited crystal is placed in a fresh 0.1 M HEPES solution (pH 7.0) devoid of inhibitor, approximately half of the intermediate remains associated with the protein crystal for at least 24 h. Using several crystals, we estimate that the reproducibility of the absolute intensities is ±12%. In Figure 6, the time dependence curves are normalized to the amide I band intensity, which reflects the protein concentration in the sample volume. Tazobactam seems to form the most enamine intermediate, consistent with the fact that tazobactam is the most efficient inhibitor. This behavior could, however, be due to the fact that there are subtle differences in the structure of the three enamines and that tazobactam gives rise to an intermediate that is a better Raman scatterer. The data in Figure 6 show that sulbactam has the fastest onset of the maximum enamine population in the crystal (10 min) compared to tazobactam (29 min) and clavulanic acid (22 min). However, the enamine form derived from sulbactam also decays more quickly.

It is obviously of interest to compare the kinetics of enamine formation in crystals with that for the free enzyme in aqueous solution. Since the enamine species has a characteristic absorbance near 280 nm (*7*, *11*), we were able to use changes at this wavelength to monitor the rise and fall of the enamine population in solution. For a 1:1 mixture of 40 μM tazobactam and 36 μM enzyme at pH 7.4, the maximal population was attained in <1 min, compared to 29 min in the crystal. Spontaneous hydrolysis occurred at similar rates in both the solution and crystal. For clavulanic acid (40 μM) with enzyme (36 μM) in solution, maximal enamine was observed at 5 min, compared to a value of 22 min in the crystal. Again, loss of enamine occurs at similar rates under both conditions. The slower rate of enamine formation in the crystal can be caused by a number of factors such as steric hindrance of the active site or the damping of catalytically important protein breathing modes in the crystal. However, the differences between solution and crystal kinetics appear to be fairly modest.

Our discussion above pertains exclusively to E166A SHV. However, recent Raman studies with the wild-type enzyme reveal formation of the *trans*-enamine intermediate with the inhibitors under similar conditions. These data will be the subject of a future report.

CONCLUSION

Raman crystallography has been successfully applied to study the reaction intermediates of a β-lactamase enzyme with three mechanism-based inhibitors. We have demonstrated the structure and kinetic behavior of a critical intermediate, *trans*-enamine, on the reaction pathway. This provides exquisite control for X-ray crystallographic studies where specific intermediates can be trapped by flash-freezing. Furthermore, future studies utilizing clinically relevant mutant β-lactamases open the door to the molecular origins of drug resistance.

SUPPORTING INFORMATION AVAILABLE

Solution Raman difference spectrum of E166A SHV with tazobactam 20 min after mixing (Figure 1), where the solution *S*/*N* ratio is 20/1 and the signal/background ratio is 0.5/1 for the amide I band (in β-lactamase crystals, the *S*/*N* ratio is 400/1 and the signal/background ratio 13/1); Raman difference spectrum of Meropenem and E166A SHV in H_2O (Figure 2); and time dependence of the 1552 cm^{-1} signal of Meropenem (Figure 3). This material is available free of charge via the Internet at http://pubs.acs.org.

REFERENCES

1. Fisher, J., Charnas, R. L., and Knowles, J. R. (1978) *Biochemistry 17*, 2180−2184.
2. Charnas, R. L., Fisher, J., and Knowles, J. R. (1978) *Biochemistry 17*, 2185−2189.
3. Fisher, J., Belasco, J. G., Charnas, R. L., Khosla, S., and Knowles, J. R. (1980) *Philos. Trans. R. Soc. London, Ser. B 289*, 309−319.
4. Charnas, R. L., and Knowles, J. R. (1981) *Biochemistry 20*, 3214−3219.
5. Brenner, D. G., and Knowles, J. R. (1981) *Biochemistry 20*, 3680−3687.
6. Fisher, J., Charnas, R. L., Bradley, S. M., and Knowles, J. R. (1981) *Biochemistry 20*, 2726−2731.
7. Kemal, C., and Knowles, J. R. (1981) *Biochemistry 20*, 3688−3695.
8. Brenner, D. G., and Knowles, J. R. (1984) *Biochemistry 23*, 5839−5846.
9. Brenner, D. G., and Knowles, J. R. (1984) *Biochemistry 23*, 5833−5839.
10. Brown, R. P. A., Aplin, R. T., and Schofield, C. J. (1996) *Biochemistry 35*, 12421−12432.
11. Bush, K., Clarissa, M., Rasmussen, B. A., Lee, V. J., and Yang, Y. (1993) *Antimicrob. Agents Chemother. 37*, 851−858.
12. Yang, Y., Janota, K., Tabei, K., Huang, N., Siegel, M. M., Lin, Y.-I., Rasmussen, B. A., and Shlaes, D. M. (2000) *J. Biol. Chem. 275*, 26674−26682.
13. Chen, C. C., and Herzberg, O. (1992) *J. Mol. Biol. 224*, 1103−1113.
14. Kuzin, A. P., Michiyoshi, N., Michiyoshi, Y., Hujer, A. M., Bonomo, R. A., and Knox, J. R. (2001) *Biochemistry 40*, 1861−1866.
15. Carey, P. R. (1999) *J. Biol. Chem. 274*, 26625−26628.
16. Dong, J., Swift, K., Matayoshi, E., Nienaber, V. L., Weitzberg, M., Rockway, T., and Carey, P. R. (2001) *Biochemistry 40*, 9751−9757.

17. Hujer, A. M., Hujer, K. M., and Bonomo, R. A. (2001) *Biochim. Biophys. Acta 1547*, 37−50.
18. Helfand, M. S., Hujer, A. M., Sonnichsen, F. D., and Bonomo, R. A. (2002) *J. Biol. Chem. 277*, 47719−47723.
19. Kuzin, A. P., Michiyoshi, N., Michiyoshi, Y., Hujer, A. M., Bonomo, R. A., and Knox, J. R. (1999) *Biochemistry 38*, 5720−5727.
20. Glasoe, P. K., and Long, F. A. (1960) *J. Phys. Chem. 64*, 88−90.
21. Altose, M. D., Zheng, Y., Dong, J., Palfey, B. A., and Carey, P. R. (2001) *Proc. Natl. Acad. Sci. U.S.A. 98*, 3006−3011.
22. Frisch, M. J., Trucks, G. W., Schlegel, H. B., Scuseria, G. E., and Pople, J. A. (1998) *Gaussian 98*, Gaussian, Pittsburgh, PA.
23. Harada, I., and Takeuchi, H. (1986) in *Spectroscopy of Biological Systems* (Clark, R. J. H., and Hester, R. E., Eds.) pp 113−175.

BI035716W